PHYSICAL REVIEW D **86,** 015021 (2012)

# A Higgs conundrum with vector fermions

S. Dawson and E. Furlan

*Department of Physics, Brookhaven National Laboratory, Upton, New York 11973, USA*

(Received 24 May 2012; published 20 July 2012)

Many models of beyond the standard model physics involve heavy colored fermions. We study models where the new fermions have vector interactions and examine the connection between electroweak precision measurements and Higgs production. In particular, for parameters that are allowed by precision measurements, we show that the gluon fusion Higgs cross section and the Higgs decay branching ratios must be close to those predicted by the standard model. The models we discuss thus represent scenarios with new physics that will be extremely difficult to distinguish from the minimal standard model. We pay particular attention to the decoupling properties of the vector fermions.

DOI: 10.1103/PhysRevD.86.015021 PACS numbers: 12.60.−i, 14.65.Ha, 14.65.Jk, 14.80.Bn

## I. INTRODUCTION

The standard model of particle physics has a remarkable body of experimental support, but the Higgs boson remains a missing ingredient. Precision electroweak measurements suggest that a standard model Higgs boson must be lighter than ∼145 GeV [1,2] and recent measurements from the LHC exclude a standard model Higgs boson in the range 129 GeV $< M_H <$ 600 GeV [3]. Preliminary measurements suggest a light Higgs boson in the mass region $M_H \sim 125$ GeV [3,4]. Should this putative Higgs signal be confirmed, the pressing issue will be understanding its properties.

For all Higgs masses, gluon fusion is the dominant production mechanism at hadron colliders and the production rate is well understood up to next-to-next-to leading order (NNLO) in QCD [5,6]. Theoretical uncertainties from renormalization/factorization scale choices and from the choice of parton distribution functions are also well understood [7–10]. The total rate, however, is sensitive to the existence of colored particles that couple to the Higgs boson. Beyond the standard model physics can potentially have a large effect on the Higgs boson production rate, making this a window to high scale physics [8,11–13].

The effects on Higgs production of squarks, Kaluza Klein colored fermions, color octet scalars, fermionic top quark partners and 4th generation fermions (among many others) have been extensively studied. The simplest possibility for new heavy fermions is to form a chiral heavy new generation that, except for masses, is an exact copy of the known generations. After careful tuning, it is possible to find combinations of 4th generation fermion masses that are permitted by precision electroweak measurements [14,15] and are not excluded by direct searches. Since a chiral 4th generation quark is assumed to couple to the Higgs boson with a strength proportional to its mass, heavy quarks do not decouple from the production of the Higgs boson (and in fact increase the rate by a factor of ∼9). The existence of a 4th generation of fermions would exclude a Higgs boson mass up to $M_H \sim 600$ GeV [16] regardless of the fermion masses.

In this paper, we study the effect of heavy vector quarks on Higgs boson production and study both the case of an isospin singlet top partner and an isospin doublet of heavy fermions. A vector singlet top partner arises naturally in little Higgs models [17–23], where the couplings to the Higgs boson of the top quark and its fermion partner are fixed in such a manner as to cancel their quadratically divergent contributions to the Higgs mass renormalization. Top-quark fermion partners are also found in top color [24,25] and top condensate [26–29] models where there is a natural hierarchy of scales such that the top partner obtains a large Dirac mass. Light vector fermions instead typically appear in composite Higgs models [30–33]. Our results are general enough to be applied to any of these models and hence represent a simplification of results that have previously been presented in the context of very specific scenarios.

A study of the $S$, $T$, $U$ parameters and the $Z \to b\bar{b}$ decay rate [34,35] restricts the allowed parameter space for heavy vector fermions. However, vector fermions have interesting decoupling properties as the mixing with the standard model fermions becomes small, which makes a large region of parameter space experimentally viable. Vector fermions that couple to the standard model fermions and Higgs boson can be $SU(2)_L$ singlets with the same hypercharge as the standard model right-handed quarks, doublets with $Y = Y_{\rm SM} = \frac{1}{6}$ or $Y = Y_{\rm SM} \pm 1$, or triplets with $Y = Y_{\rm SM} \pm \frac{1}{2}$ [36]. We consider the "standard model-like" case with either a heavy fermion singlet of charge $2/3$ or a doublet with the standard model assignments of hypercharge. We compute the NNLO prediction for Higgs production for the allowed parameter region of these models and quantify the allowed deviation from the standard model prediction. The new features of our study include up-to-date fits to precision electroweak measurements in models with vector fermions, and an analysis of the resulting consequences for Higgs boson production at NNLO in perturbative QCD.

 

## II. THE MODELS

We consider models with additional vectorlike charge $2/3$ quarks, $\mathcal{T}^\alpha$, and charge $-1/3$ quarks, $\mathcal{B}^\alpha$, that mix with the standard model-like third generation quarks. For simplicity we make the following assumptions:

(i) the electroweak gauge group is the standard $SU(2)_L \times U(1)_Y$ group;

(ii) there is only a single standard model Higgs $SU(2)_L$ doublet,

$$H = \begin{pmatrix} \phi^+ \\ \phi^0 \end{pmatrix}, \tag{1}$$

with $\phi^0 = \frac{v+h}{\sqrt{2}}$;

(iii) we neglect generalized Cabibbo-Kobayashi-Maskawa (CKM) mixing and only allow mixing between the standard model-like third generation quarks and at most one new charge $2/3$ quark singlet or one new $SU(2)_L$ quark doublet. We do not consider fermions in more exotic representations.

The standard model-like chiral fermions are

$$\psi_L^1 = \begin{pmatrix} \mathcal{T}_L^1 \\ \mathcal{B}_L^1 \end{pmatrix}, \qquad \mathcal{T}_R^1, \mathcal{B}_R^1, \tag{2}$$

with the Lagrangian describing the fermion masses

$$-\mathcal{L}_M^{\rm SM} = \lambda_1 \bar{\psi}_L^1 H \mathcal{B}_R^1 + \lambda_2 \bar{\psi}_L^1 \tilde{H} \mathcal{T}_R^1 + \text{H.c.}, \tag{3}$$

and $\tilde{H} = i\sigma_2 H^*$.

The models we consider are

(i) singlet fermion model: add a vector $SU(2)_L$ quark singlet of charge $2/3$, $\mathcal{T}_L^2$, and $\mathcal{T}_R^2$.

(ii) doublet fermion model: add a vector $SU(2)_L$ doublet of hypercharge $1/6$,

$$\psi_L^2 = \begin{pmatrix} \mathcal{T}_L^2 \\ \mathcal{B}_L^2 \end{pmatrix}, \qquad \psi_R^2 = \begin{pmatrix} \mathcal{T}_R^2 \\ \mathcal{B}_R^2 \end{pmatrix}. \tag{4}$$

## III. EXPERIMENTAL LIMITS ON TOP PARTNER MODELS

### A. Limits from $R_b$ and $A_b$

Data from LEP and SLD place stringent restrictions on the couplings of the fermionic top partners. The top partners mix with the standard model-like top quark and contribute at one-loop to processes involving bottom quarks, especially $Z \to b\bar{b}$ and $A_b$. The neutral current couplings to the bottom can be parametrized by the effective Lagrangian

$$\mathcal{L}^{\rm NC} = \frac{g}{c_W} Z_\mu \bar{f} \gamma^\mu \Big[ (g_L^f + \delta\tilde{g}_L^f)\Big(\frac{1-\gamma_5}{2}\Big) + (g_R^f + \delta\tilde{g}_R^f)\Big(\frac{1+\gamma_5}{2}\Big)\Big] f, \tag{5}$$

where the standard model couplings are normalized such that $g_L^f = T_3^f - Q_f s_W^2$, $g_R^f = -Q_f s_W^2$, with $s_W^2 \equiv \sin^2\theta_W = (e/g)^2 = 0.231$ [37] and $T_3^f = \pm 1/2$. The couplings $\delta\tilde{g}_{L,R}^f \equiv \delta g_{L,R}^{f,\rm SM} + \delta g_{L,R}^f$ contain both the standard model radiative corrections, $\delta g_{L,R}^{f,\rm SM}$, and the new physics contributions, $\delta g_{L,R}^f$. The standard model contribution from top quark loops is well known [38–40], and in the limit $m_t \gg M_Z$ it is given by

$$\delta g_L^{b,\rm SM} = \frac{G_F}{\sqrt{2}} \frac{m_t^2}{8\pi^2}. \tag{6}$$

The dominant effect of new physics in the $b$ sector can be found by assuming that $\delta g_L^b$ and $\delta g_R^b$ are small and approximating [41,42]

$$R_b = \frac{\Gamma(Z \to b\bar{b})}{\Gamma(Z \to \text{hadrons})} = R_b^{\rm SM}\Big\{1 - 3.57\delta g_L^b + 0.65\delta g_R^b\Big\}$$
$$A_b = \frac{(\delta\tilde{g}_L^b)^2 - (\delta\tilde{g}_R^b)^2}{(\delta\tilde{g}_L^b)^2 + (\delta\tilde{g}_R^b)^2} = A_b^{\rm SM}\Big\{1 - 0.31\delta g_L^b - 1.72\delta g_R^b\Big\}, \tag{7}$$

where $R_b^{\rm SM}$ and $A_b^{\rm SM}$ are the theory predictions including all radiative corrections. The positive contribution to $\delta g_L^{b,\rm SM}$ from the top quark has the effect of reducing both $R_b^{\rm SM}$ and $A_b^{\rm SM}$.

The 95% confidence level ellipse for new $Zb\bar{b}$ couplings is shown in Fig. 1 and is obtained using the Particle Data Group results [37,43]

$$R_b^{\rm exp} = 0.21629 \pm 0.00066, \quad R_b^{\rm SM} = 0.21578 \pm 0.00005,$$
$$A_b^{\rm exp} = 0.923 \pm 0.020, \quad A_b^{\rm SM} = 0.9348 \pm 0.0001. \tag{8}$$

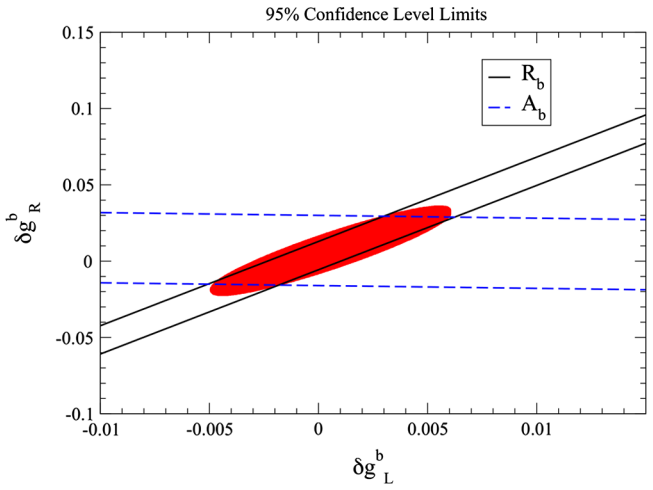


FIG. 1 (color online). Allowed 95% confidence level regions from the simultaneous fit to $R_b$ and $A_b$ (red shaded), $R_b$ alone (between solid black lines), and $A_b$ alone (between dashed blue lines).

If $\delta g_R^b = 0$, the 95% confidence level limit from the fit to $A_b$ and $R_b$ is

$$-0.0027 < \delta g_L^b < 0.0014. \quad (9)$$

Similarly, if $\delta g_L^b = 0$, the 95% confidence level limit from the fit to $A_b$ and $R_b$ is

$$-0.0066 < \delta g_R^b < 0.0148. \quad (10)$$

### B. Limits from the oblique parameters $S$, $T$, and $U$

The new quarks contribute at loop level to the vacuum polarizations of the electroweak gauge bosons $\Pi_{XY}^{\mu\nu}(p^2) = \Pi_{XY}(p^2) g^{\mu\nu} + B_{XY}(p^2) p^\mu p^\nu$, with $XY = \gamma\gamma, \gamma Z, ZZ$ and $W^+W^-$ [44,45]. These effects can be parametrized using the $S$, $T$, and $U$ functions of Peskin and Takeuchi [44],

$$\begin{aligned}
\alpha S_F &= \frac{4 s_W^2 c_W^2}{M_Z^2}\left\{\Pi_{ZZ}(M_Z^2) - \Pi_{ZZ}(0) - \Pi_{\gamma\gamma}(M_Z^2) \right. \\
&\quad \left. - \frac{c_W^2 - s_W^2}{c_W s_W}\Pi_{\gamma Z}(M_Z^2)\right\}, \\
\alpha T_F &= \frac{\Pi_{WW}(0)}{M_W^2} - \frac{\Pi_{ZZ}(0)}{M_Z^2}, \\
\alpha U_F &= 4 s_W^2 \left\{\frac{\Pi_{WW}(M_W^2) - \Pi_{WW}(0)}{M_W^2}\right. \\
&\quad - c_W^2\left(\frac{\Pi_{ZZ}(M_Z^2) - \Pi_{ZZ}(0)}{M_Z^2}\right) - 2 s_W c_W \frac{\Pi_{\gamma Z}(M_Z^2)}{M_Z^2} \\
&\quad \left. - s_W^2 \frac{\Pi_{\gamma\gamma}(M_Z^2)}{M_Z^2}\right\}. \quad (11)
\end{aligned}$$

Any definition of $s_W$ can be used in Eq. (11) since the scheme dependence enters at higher order. Since these parameters are well constrained by LEP and LEP2 measurements [46], they set stringent limits on the masses and couplings of the new quarks.

We use the fit to the electroweak precision data given in Refs. [2,47],

$$\begin{aligned}
\Delta S &= S - S_{\rm SM} = 0.02 \pm 0.11, \\
\Delta T &= T - T_{\rm SM} = 0.05 \pm 0.12, \quad (12) \\
\Delta U &= U - U_{\rm SM} = 0.07 \pm 0.12,
\end{aligned}$$

with reference Higgs and top quark masses $M_{H,\rm ref} = 120$ GeV and $m_{t,\rm ref} = 173.1$ GeV. The associated correlation matrix is

$$\rho_{ij} = \begin{pmatrix} 1.0 & 0.879 & -0.469 \\ 0.879 & 1.0 & -0.716 \\ -0.469 & -0.716 & 1.0 \end{pmatrix}.$$

The $\Delta\chi^2$ is defined as

$$\Delta\chi^2 = \sum_{i,j} (\Delta X_i - \Delta\hat{X}_i)(\sigma^2)_{ij}^{-1}(\Delta X_j - \Delta\hat{X}_j), \quad (13)$$

where $\Delta\hat{X}_i = \Delta S, \Delta T$, and $\Delta U$ are the central values of the fit in Eq. (12), $\Delta X_i = X_i - X_i^{\rm SM} = \Delta S_F, \Delta T_F$ and $\Delta U_F$ are the contributions to the oblique parameters from the new fermions, and $\sigma_{ij}^2 \equiv \sigma_i \rho_{ij} \sigma_j$, $\sigma_i$ being the errors given in Eq. (12). A 95% confidence level limit in a three-parameter fit corresponds to $\Delta\chi^2 = 7.82$.

Since we consider primarily $M_H = 125$ GeV, we need to add the Higgs contributions[1]

$$\begin{aligned}
\Delta S_H &= \frac{1}{12\pi}\log\left(\frac{M_H^2}{M_{H,\rm ref}^2}\right) + \mathcal{O}\left(\frac{M_Z^2}{M_H^2}\right), \\
\Delta T_H &= -\frac{3}{16\pi c_W^2}\log\left(\frac{M_H^2}{M_{H,\rm ref}^2}\right) + \mathcal{O}\left(\frac{M_Z^2}{M_H^2}\right), \quad (14) \\
\Delta U_H &= \mathcal{O}\left(\frac{M_Z^2}{M_H^2}\right).
\end{aligned}$$

### C. Other experimental limits on top partner models

Both ATLAS [50,51] and CMS [52,53] have searched for direct pair production of new heavy fermions. For charge $2/3$ toplike quarks decaying with 100% branching ratio to $Wb$, CMS excludes masses below 557 GeV at 95% confidence level, while ATLAS sets an upper bound of 404 GeV. CMS dedicates a specific analysis to pair-produced vector quarks of charge $2/3$ decaying entirely to $Zt$, excluding masses below 475 GeV [54]. For charge $-1/3$ quarks, assuming 100% branching ratio to $Zb$, ATLAS excludes masses below 358 GeV for a vector singlet, while CMS excludes charge $-1/3$ quarks decaying with 100% branching ratio to $Wt$ below 611 GeV. These limits are not directly applicable to our models, since the branching ratios of the new heavy fermions to standard model particles are degraded by mixing angles and the limits therefore weakened [36,55–59]. Our results on Higgs production are rather insensitive to the masses of the new top partners and we typically assume masses of the TeV scale.

In principle, there are also limits on heavy charged fermions that mix with the standard model third generation quarks coming from $K$, $B$, and $D$ rare processes. For TeV-scale masses of the new fermions and small mixing parameters (which we will see in the next section are required by limits from oblique parameters, $R_b$ and $A_b$), the constraints from rare processes are not restrictive [57,59–61].

## IV. SINGLET TOP PARTNER MODEL

Little Higgs models [17–23], topcolor models [24,25], and top condensate models [26–28] all contain a charge $2/3$ partner of the top quark, which we denote by $\mathcal{T}^2$. We consider a general case with a vector $SU(2)_L$ singlet fermion that is allowed to mix with the standard

[1]Our fits include the exact results for the Higgs contributions, which can be found in many places including Ref. [48] and the appendix of Ref. [49].

model-like top quark [19,36,60,62,63]. The mass eigenstates are $b \equiv \tilde{\mathcal{B}}^1$, $t$, and $T$, where $b$ and $t$ are the observed bottom and top quarks. Thorough this paper we will use the measured mass values $m_b = 4.19$ GeV, $m_t = 173.1$ GeV [37,64]. The mass eigenstates of charge 2/3 can be found through the rotations

$$\chi^t_{L,R} \equiv \begin{pmatrix} t_{L,R} \\ T_{L,R} \end{pmatrix} \equiv U^t_{L,R} \begin{pmatrix} \mathcal{T}^1_{L,R} \\ \mathcal{T}^2_{L,R} \end{pmatrix}. \tag{15}$$

The matrices $U^t_{L,R}$ are unitary and $\Psi_{L,R} \equiv \frac{1\mp\gamma_5}{2}\Psi$. The mixing matrices are parametrized as

$$\begin{aligned} U^t_L &= \begin{pmatrix} \cos\theta_L & -\sin\theta_L \\ \sin\theta_L & \cos\theta_L \end{pmatrix}, \\ U^t_R &= \begin{pmatrix} \cos\theta_R & -\sin\theta_R \\ \sin\theta_R & \cos\theta_R \end{pmatrix}. \end{aligned} \tag{16}$$

We abbreviate $c_L \equiv \cos\theta_L$, $s_L \equiv \sin\theta_L$.

The most general fermion mass terms are

$$\begin{aligned} -\mathcal{L}_{M,1} &= -\mathcal{L}^{\rm SM}_M + \lambda_3 \bar{\psi}^1_L \tilde{H} \mathcal{T}^2_R + \lambda_4 \bar{\mathcal{T}}^2_L \mathcal{T}^1_R \\ &\quad + \lambda_5 \bar{\mathcal{T}}^2_L \mathcal{T}^2_R + \text{H.c.} \\ &= \bar{\chi}^t_L [U^t_L (M^t_{(1)} + h H^t_{(1)}) U^{t,\dagger}_R] \chi^t_R \\ &\quad + \lambda_1 \frac{v+h}{\sqrt{2}} \bar{\mathcal{B}}^1_L \mathcal{B}^1_R + \text{H.c.}, \end{aligned} \tag{17}$$

where

$$M^t_{(1)} = \begin{pmatrix} \lambda_2 \frac{v}{\sqrt{2}} & \lambda_3 \frac{v}{\sqrt{2}} \\ \lambda_4 & \lambda_5 \end{pmatrix}, \quad H^t_{(1)} = \frac{1}{\sqrt{2}} \begin{pmatrix} \lambda_2 & \lambda_3 \\ 0 & 0 \end{pmatrix}. \tag{18}$$

The resulting mass eigenstates are

$$\mathcal{M}^{t,\rm diag} \equiv \begin{pmatrix} m_t & 0 \\ 0 & M_T \end{pmatrix}. \tag{19}$$

One can always rotate $\mathcal{T}^2$ such that $\lambda_4 = 0$. Since $\lambda_4$ can be rotated away, the model has four free parameters. Alternatively, it is always possible to rotate $\mathcal{T}^2_R$ such that $\sin\theta_R = 0$, because only the standard model-like left-handed doublet $\psi^1_L$ mixes to the singlet with a Yukawa term.[2] Therefore, the couplings only depend on $\theta_L$, which we will take as one of the four physical parameters along with $m_b$ (physical mass of the charge $-1/3$ quark), $m_t$ and $M_T$ (physical masses of the charge 2/3 quarks).

The physical masses and mixing angles are found using bi-unitary transformations,

$$(\mathcal{M}^{t,\rm diag})^2 = U^t_L M^t_{(1)} M^{t,\dagger}_{(1)} U^{t,\dagger}_L = U^t_R M^{t,\dagger}_{(1)} M^t_{(1)} U^{t,\dagger}_R. \tag{20}$$

[2]We do not perform any of these rotations here, and the formulas in this section hold for the arbitrary Yukawa couplings of Eq. (17).

It is straightforward to find the mass eigenstates and mixing angles,

$$\begin{aligned} \tan(2\theta_R) &= \frac{2\lambda_4\lambda_5 + v^2\lambda_2\lambda_3}{\lambda_5^2 - \lambda_4^2 + \frac{v^2}{2}(\lambda_3^2 - \lambda_2^2)}, \\ \tan(2\theta_L) &= \frac{\sqrt{2}v(\lambda_2\lambda_4 + \lambda_3\lambda_5)}{\lambda_5^2 + \lambda_4^2 - \frac{v^2}{2}(\lambda_2^2 + \lambda_3^2)}, \\ m_t M_T &= \frac{v}{\sqrt{2}} \mid \lambda_2\lambda_5 - \lambda_3\lambda_4 \mid, \\ M_T^2 + m_t^2 &= \frac{v^2}{2}(\lambda_2^2 + \lambda_3^2) + \lambda_4^2 + \lambda_5^2. \end{aligned} \tag{21}$$

From Eq. (17), the couplings to the Higgs boson are

$$\begin{aligned} \mathcal{L}^h_1 &= -\frac{m_t}{v} c_{tt} \bar{t}_L t_R h - \frac{M_t}{v} c_{TT} \bar{T}_L T_R h - \frac{M_t}{v} c_{tT} \bar{t}_L T_R h \\ &\quad - \frac{m_t}{v} c_{Tt} \bar{T}_L t_R h + \text{H.c.}, \end{aligned} \tag{22}$$

where

$$c_{tt} = c_L^2, \qquad c_{TT} = s_L^2, \qquad c_{tT} = c_{Tt} = s_L c_L. \tag{23}$$

These relations can be easily derived by noticing that

$$v H^t_{(1),ks} = M^t_{(1),ks} \delta_{k1}, \tag{24}$$

yielding for the physical Higgs couplings

$$\begin{aligned} H_{ij} &\equiv U^t_{L,ik} H^t_{(1),ks} U^{t,\dagger}_{R,sj} \\ &= v^{-1} U^t_{L,i\hat{k}} \delta_{\hat{k}1} [U^{t,\dagger}_{L,\hat{k}r} \mathcal{M}^{t,\rm diag}_{rr} U^t_{R,rs}] U^{t,\dagger}_{R,sj} \\ &= v^{-1} U^t_{L,i\hat{k}} \delta_{\hat{k}1} U^{t,\dagger}_{L,\hat{k}j} \mathcal{M}^{t,\rm diag}_{jj}, \end{aligned} \tag{25}$$

where the index $\hat{k}$ is not summed over.

The charged and neutral current interactions are

$$\mathcal{L}^{CC}_1 = \frac{g}{\sqrt{2}} W^{\mu+} \sum_{i=1,2} (\bar{\chi}^t_L)_i (U^t_L)_{i,1} \gamma_\mu b_L + \text{H.c.} \tag{26}$$

and

$$\begin{aligned} \mathcal{L}^{NC}_1 &= \frac{g}{c_W} Z_\mu \sum_{i=t,T} \{\bar{f}_i \gamma^\mu [(g^i_L + \delta\tilde{g}^i_L) P_L + (g^i_R + \delta\tilde{g}^i_R) P_R] f_i\} \\ &\quad + \frac{g}{c_W} Z_\mu \sum_{i\neq j} \{\bar{f}_i \gamma^\mu [\delta g^{ij}_L P_L + \delta g^{ij}_R P_R] f_j\}, \end{aligned} \tag{27}$$

where $\delta\tilde{g}^i_{L,R} = \delta g^{i,\rm SM}_{L,R} + \delta g^i_{L,R}$ contains both the standard model contribution from top quark loops and the new physics contributions. The new physics couplings arising from the interactions of the top partner singlet are

$$\begin{aligned} &\delta g^t_L = -\frac{s_L^2}{2}, \qquad \delta g^T_L = -\frac{c_L^2}{2}, \qquad \delta g^{tT}_L = \frac{s_L c_L}{2}, \\ &\delta g^i_R = \delta g^{ij}_R = 0, \qquad i,j = t,T. \end{aligned} \tag{28}$$

Finally, the unitarity bound from the scattering $T\bar{T} \to T\bar{T}$ is modified from the standard model limit and becomes [65,66]

$$M_T(\text{Unitarity Bound}) \lesssim \frac{550\ \text{GeV}}{s_L^2}. \tag{29}$$

This class of models therefore allows quite heavy $T$ quarks without violating perturbative unitarity.

### Experimental restrictions on singlet top partner model

Using the results given above, it is straightforward to compute the contributions to the $S$, $T$, and $U$ parameters in the singlet top partner model. Expressions for the gauge boson two-point functions for arbitrary fermion couplings are given in the Appendix [21,67,68], and we assume $M_T \gg M_Z$. Subtracting the standard model $t-b$ loops, the new contributions are

$$\begin{aligned}
\Delta T_F &= T_{\text{SM}} s_L^2 \Big[ -(1+c_L^2) + s_L^2 r + 2c_L^2 \frac{r}{r-1}\log(r) \\
&\quad + \mathcal{O}\Big(\frac{M_Z^2}{m_t^2}, \frac{M_Z^2}{M_T^2}, \frac{m_b^2}{m_t^2}\Big)\Big], \\
\Delta S_F &= -\frac{N_C}{18\pi} s_L^2 \Big\{ \log(r) + c_L^2 \Big[ \frac{5(r^2+1)-22r}{(r-1)^2} \\
&\quad + \frac{3(r+1)(r^2-4r+1)}{(1-r)^3}\log(r) \Big] \\
&\quad + \mathcal{O}\Big(\frac{M_Z^2}{m_t^2}, \frac{M_Z^2}{M_T^2}, \frac{m_b^2}{m_t^2}\Big)\Big\}, \\
\Delta S_F + \Delta U_F &= \frac{N_C}{9\pi} s_L^2 \Big[ \log(r) + \mathcal{O}\Big(\frac{M_Z^2}{m_t^2}, \frac{M_Z^2}{M_T^2}, \frac{m_b^2}{m_t^2}\Big)\Big],
\end{aligned} \tag{30}$$

where

$$r \equiv \frac{M_T^2}{m_t^2}, \quad N_C = 3, \text{ and } T_{\text{SM}} = \frac{N_C}{16\pi s_W^2}\frac{m_t^2}{M_W^2} \tag{31}$$

is the $t-b$ contribution to the $T$ parameter in the limit of a massless bottom quark. We use $M_W = 80.4$ GeV, $M_Z = 91.2$ GeV [37]. Equation (30) agrees with the $m_b \to 0$ and $M_Z \ll M_T, m_t$ limits of Refs. [69–71].[3] For a top partner much heavier than the top quark, $M_T \gg m_t$, the oblique parameters take simple forms,

$$\begin{aligned}
\Delta T_F(\text{approx}) &= T_{\text{SM}} s_L^2 [-(1+c_L^2) + s_L^2 r + 2c_L^2 \log(r)], \\
\Delta S_F(\text{approx}) &= -\frac{N_C}{18\pi} s_L^2 [5c_L^2 + (1-3c_L^2)\log(r)].
\end{aligned} \tag{32}$$

One would expect decoupling to occur for a very heavy vector top partner, i.e. for $r \to \infty$. From Eqs. (30) and (32), instead, the effects of the top partner on the oblique parameters vanish only in the limit $s_L \to 0$. This can be understood inspecting the mass matrix (18): to obtain decoupling both the Yukawa interactions and the off-diagonal terms need to be small, $\lambda_2 v,\ \lambda_3 v,\ \lambda_4 \ll \lambda_5$. In this limit

$$s_L \to \frac{v\lambda_3}{\sqrt{2}M_T} + \frac{\lambda_2\lambda_4 v}{\sqrt{2}M_T^2} + \ldots \tag{33}$$

and the top partner effects vanish for large $M_T$, as expected.

In Fig. 2 we show the oblique parameters for a fixed $M_T = 1$ TeV. It is clear that the approximate forms of Eq. (32) are excellent approximations to the complete results for mass values of this order. The largest contribution is to $\Delta T_F$ due to the large isospin violation for nonzero $\sin\theta_L$. In this case, the isospin violation is manifest in the result that $\Delta U_F > \Delta S_F$. The new physics effects vanish as $s_L \to 0$ and we recover the standard model couplings. The oblique parameters for fixed $\sin\theta_L$ are shown in Figs. 3 and 4 as a function of $M_T$. As we argued, the decoupling does not occur for large $M_T$, but requires $s_L \to 0$.

The parameter space allowed by a fit to the oblique parameters can be found using the results of Sec. III. Figure 5 shows the 95% confidence level upper bound on the mixing angle $\sin\theta_L$ as a function of $M_T$ for a light Higgs boson. For a heavier Higgs boson, it is possible to use the positive contribution to $T$ from the top partner to compensate for the negative contribution from the heavy Higgs, as shown in Fig. 6. In this case, a minimum degree of mixing is required, since such a heavy Higgs boson is excluded by the electroweak fit in the three-generation standard model. The heavier the Higgs boson, the smaller the range of $\sin\theta_L$ allowed. This situation was explored for an extremely heavy Higgs boson ($M_H \sim 800$ GeV) in Ref. [72].

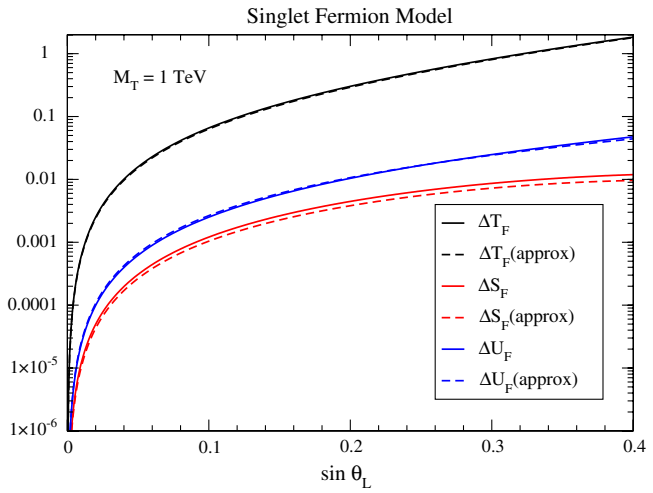


FIG. 2 (color online). Contributions to $\Delta T_F$, $\Delta S_F$, $\Delta U_F$ from a singlet top partner as a function of $\sin\theta_L$ for fixed $M_T = 1$ TeV. The results of Eq. (32) in the limit $M_T \gg m_t$ are shown as $\Delta T_F(\text{approx})$, $\Delta S_F(\text{approx})$, and $\Delta U_F(\text{approx})$.

[3]There is a typo in Eq. 88 of Ref. [70], where there is a 2 instead of the factor 22 in Eq. (30).

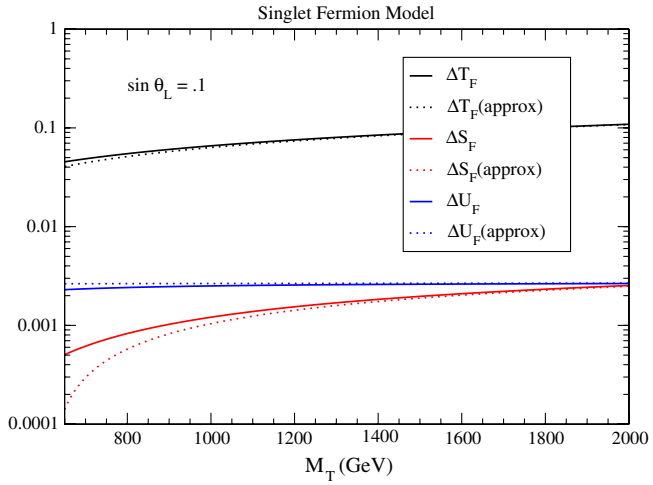


FIG. 3 (color online). Fermion contributions to $\Delta T_F$, $\Delta S_F$, $\Delta U_F$ in the singlet top partner model for fixed $\sin\theta_L = 0.1$. The dotted lines represent the approximate results from Eq. (32) in the limit $M_T \gg m_t$.

The mixing in the charge 2/3 sector also affects $R_b$. In the limit $m_b \to 0$ and neglecting the small correlations between $R_b$ and the oblique parameters, only $\delta g_L^b$ is affected by the singlet top partner. Its contribution to $\delta g_L^b$ can be found from the general analysis of Ref. [73],

$$\delta g_L^b = \frac{g^2}{64\pi^2} s_L^2 (f_1(x,x') + c_L^2 f_2(x,x')), \tag{34}$$

where $x = m_t^2/M_W^2$ and $x' = M_T^2/M_W^2$. The standard model top contribution has been subtracted following the definition of Eq. (5). In the heavy mass limit, $x, x' \gg 1$,

$$f_1(x,x') = x' - x + 3\log\left(\frac{x'}{x}\right),$$
$$f_2(x,x') = -x - x' + \frac{2xx'}{x'-x}\log\left(\frac{x'}{x}\right). \tag{35}$$

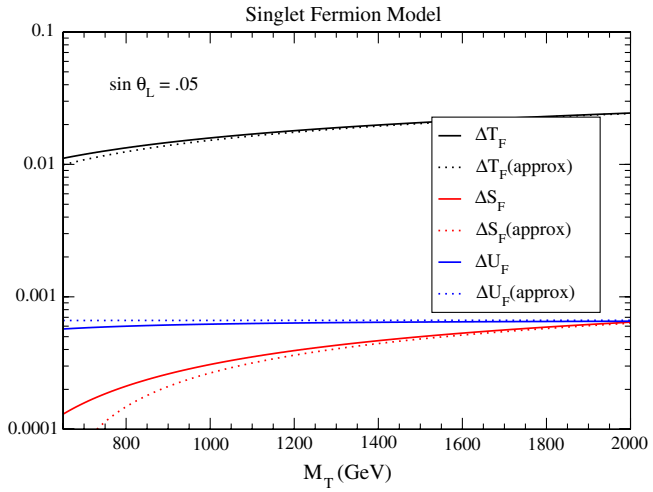


FIG. 4 (color online). Same as Fig. 3 for a smaller $\sin\theta_L = 0.05$.

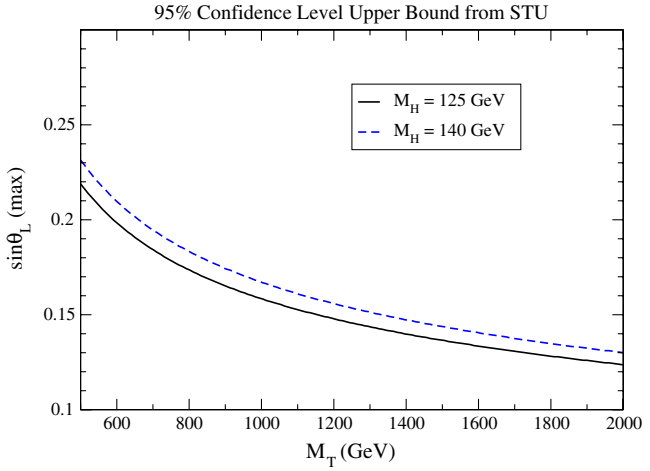


FIG. 5 (color online). 95% confidence level upper bound on the mixing angle $\sin\theta_L$ in the singlet top partner model from experimental restrictions on the $S$, $T$, and $U$ parameters.

The contribution to $\delta g_L^b$ from top singlet partners is shown in Fig. 7 as a function of $M_T$ for fixed $\sin\theta_L$, along with the 95% confidence level region allowed from the fit of Sec. III A. We use the exact one-loop calculation of $\delta g_L^b$ in the top singlet partner model, following Refs. [73,74]. The relatively large contributions from $R_b$ can be understood by looking at the leading terms for $m_t, M_T \gg M_W$,

$$\delta g_L^b = \delta g_L^{b,\mathrm{SM}} s_L^2 \left[ -(1 + c_L^2) + s_L^2 r + 2c_L^2 \frac{r}{r-1}\log(r) \right]. \tag{36}$$

Again we see that the heavy top partner decouples only when the parameters in the mass matrix are such that $s_L \sim \frac{v}{M_T}$. Furthermore, its contributions to $\delta g_L^b$ and

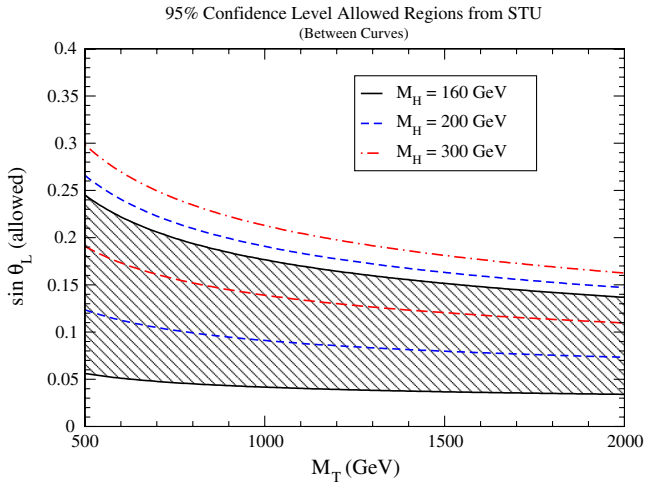


FIG. 6 (color online). 95% confidence level bands allowed by a fit to $S$, $T$, and $U$ for the mixing angle $\sin\theta_L$ in the singlet top partner model. The regions allowed are between the curves corresponding to each value of $M_H$.

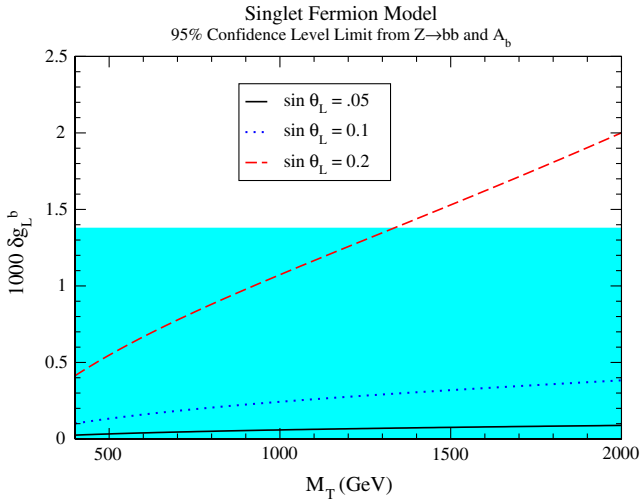


FIG. 7 (color online). Fermion contributions to $\delta g_L^b$ as a function of $M_T$ for fixed $\sin\theta_L$ in the top partner singlet model. The 95% confidence level allowed region is shaded in light blue.

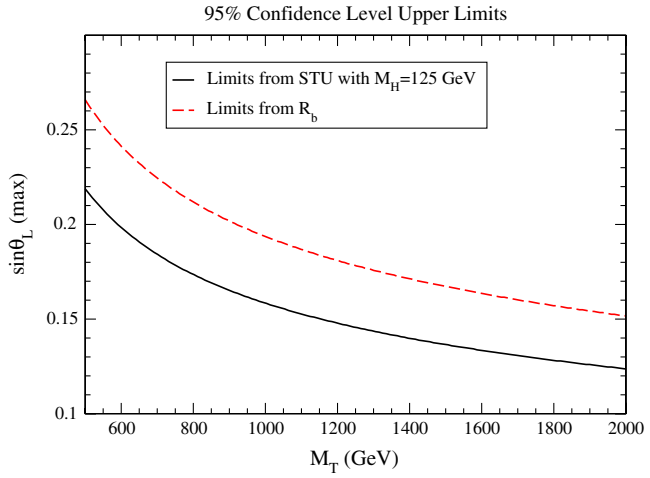


FIG. 8 (color online). Maximum allowed $\sin\theta_L$ in the top partner singlet model from oblique measurements (black solid) and $R_b$ (red dashed).

to the $T$ parameter [Eq. (32)] are both positive and strongly correlated. A large, positive contribution to $\delta g_L^b$ from the singlet also implies a large contribution to the $T$ parameter. This correlation was already pointed out in the context of composite Higgs models in Refs. [31,32,75].

Combining the new physics contribution with the standard model top quark contribution,

$$\begin{aligned}\delta\tilde{g}_L^b &= \delta g_L^{b,\mathrm{SM}} + \delta g_L^b \\ &= \delta g_L^{b,\mathrm{SM}}\left[c_L^4 + s_L^4 r + 2s_L^2 c_L^2 \frac{r}{r-1}\log(r)\right],\end{aligned} \tag{37}$$

and the net effect of the top partner is to increase $\delta\tilde{g}_L^b$ and hence reduce $R_b$.

A comparison of the maximum value of $\sin\theta_L$ allowed by the fit to $R_b$ and $A_b$ and by the experimental limits arising from the fit to $S$, $T$, and $U$ (with $M_H = 125$ GeV) is shown in Fig. 8, where it is apparent that the most stringent restrictions in the top partner singlet model come from the oblique parameters.

## V. TOP PARTNER DOUBLET

### A. Model with top partner doublet

In this section, we consider a model that has in addition to the standard model fields a vector $SU(2)_L$ doublet [36,76],

$$\psi_L^2 = \begin{pmatrix}\mathcal{T}_L^2 \\ \mathcal{B}_L^2\end{pmatrix}, \qquad \psi_R^2 = \begin{pmatrix}\mathcal{T}_R^2 \\ \mathcal{B}_R^2\end{pmatrix}. \tag{38}$$

The most general fermion mass terms allowed in the Lagrangian are

$$\begin{aligned}-\mathcal{L}_{M,2} &= -\mathcal{L}_M^{\mathrm{SM}} + \lambda_6\bar{\psi}_L^2 H\mathcal{B}_R^1 + \lambda_7\bar{\psi}_L^2\tilde{H}\mathcal{T}_R^1 \\ &\quad + \lambda_8\bar{\psi}_L^2\psi_R^2 + \lambda_9\bar{\psi}_L^1\psi_R^2 + \mathrm{H.c.} \\ &= \bar{\chi}_L^t[U_L^t M_{(2)}^t U_R^{t\dagger}]\chi_R^t + \bar{\chi}_L^b[U_L^b M_{(2)}^b U_R^{b\dagger}]\chi_R^b + \mathrm{H.c.},\end{aligned} \tag{39}$$

where $\chi_{L,R}^t$ are given by Eq. (15) and

$$\chi_{L,R}^b \equiv \begin{pmatrix}b_{L,R} \\ B_{L,R}\end{pmatrix} \equiv U_{L,R}^b\begin{pmatrix}\mathcal{B}_{L,R}^1 \\ \mathcal{B}_{L,R}^2\end{pmatrix}. \tag{40}$$

We can always rotate $\psi_2$ such that $\lambda_9 = 0$. So without loss of generality

$$M_{(2)}^t = \begin{pmatrix}\lambda_2\frac{v}{\sqrt{2}} & 0 \\ \lambda_7\frac{v}{\sqrt{2}} & \lambda_8\end{pmatrix}, \qquad M_{(2)}^b = \begin{pmatrix}\lambda_1\frac{v}{\sqrt{2}} & 0 \\ \lambda_6\frac{v}{\sqrt{2}} & \lambda_8\end{pmatrix}. \tag{41}$$

Because of the $SU(2)$ symmetry

$$M_{(2),22}^t = M_{(2),22}^b. \tag{42}$$

Diagonalizing the mass matrices now requires four unitary mixing matrices, $U_L^t$, $U_R^t$, $U_L^b$, $U_R^b$,

$$\begin{aligned}U_L^t &= \begin{pmatrix}\cos\theta_L^t & -\sin\theta_L^t \\ \sin\theta_L^t & \cos\theta_L^t\end{pmatrix}, \\ U_R^t &= \begin{pmatrix}\cos\theta_R^t & -\sin\theta_R^t \\ \sin\theta_R^t & \cos\theta_R^t\end{pmatrix}, \\ U_L^b &= \begin{pmatrix}\cos\theta_L^b & -\sin\theta_L^b \\ \sin\theta_L^b & \cos\theta_L^b\end{pmatrix}, \\ U_R^b &= \begin{pmatrix}\cos\theta_R^b & -\sin\theta_R^b \\ \sin\theta_R^b & \cos\theta_R^b\end{pmatrix}.\end{aligned} \tag{43}$$

There are five input parameters in the Lagrangian. We will take the five independent physical parameters to be the

physical masses, $m_t, M_T$ and $m_b, M_B$ (with $m_t$ and $m_b$ being the mass of the standard model-like fermions) and the right-handed mixing angle in the charge $-1/3$ sector, $\theta_R^b$. It is straightforward to find relationships among the mixing angles:

$$(\sin\theta_R^t)^2 = \frac{(\sin\theta_L^t)^2}{(\sin\theta_L^t)^2 + (\cos\theta_L^t)^2 \frac{m_t^2}{M_T^2}},$$
$$(\sin\theta_R^b)^2 = \frac{(\sin\theta_L^b)^2}{(\sin\theta_L^b)^2 + (\cos\theta_L^b)^2 \frac{m_b^2}{M_B^2}},$$
$$(\sin\theta_R^b)^2(m_b^2 - M_B^2) + M_B^2 = (\sin\theta_R^t)^2(m_t^2 - M_T^2) + M_T^2. \tag{44}$$

For small mixing, the left-handed angles are always suppressed by the heavy mass scale relative to the right-handed angles of the same charge sector,

$$\sin^2\theta_L^{t,b} \sim \frac{m_{t,b}^2}{M_{T,B}^2}\sin^2\theta_R^{t,b}. \tag{45}$$

If the mass splitting between $B$ and $T$, $\delta \equiv M_T - M_B$, is small, $\frac{|\delta|}{M_T} \ll 1$,

$$(\sin\theta_R^t)^2 = (\sin\theta_R^b)^2 + (\cos\theta_R^b)^2\frac{2\delta}{M_T} + \mathcal{O}\left(\frac{\delta^2}{M_T^2}, \frac{m_t^2}{M_T^2}, \frac{m_b^2}{M_T^2}\right). \tag{46}$$

The charged current interactions are

$$\begin{aligned}\mathcal{L}_2^{CC} &= \frac{g}{\sqrt{2}} W^{\mu+}\{[\Sigma_{i=1}^2 \bar\psi_L^i \gamma_\mu \sigma^- \psi_L^i] + \bar\psi_R^2 \gamma_\mu \sigma^- \psi_R^2\} \\ &\quad + \text{H.c.} \\ &= \frac{g}{\sqrt{2}} W^{\mu+}\{\bar X_L^t \gamma_\mu U_L^t U_L^{b,\dagger} X_L^b + \bar X_R^t \gamma_\mu U_R^t U_R^{b,\dagger} X_R^b\} \\ &\quad + \text{H.c.},\end{aligned} \tag{47}$$

where

$$\sigma^- = \begin{pmatrix} 0 & 1 \\ 0 & 0 \end{pmatrix}. \tag{48}$$

The neutral current interactions are given by Eq. (27), with

$$\begin{aligned} &\delta g_L^i = \delta g_L^{ij} = 0, \qquad i,j = t,T,b,B, \\ &\delta g_R^t = T_3^t \sin^2\theta_R^t, \qquad \delta g_R^T = T_3^T \cos^2\theta_R^t, \\ &\delta g_R^{tT} = -\tfrac{1}{2}\sin\theta_R^t\cos\theta_R^t, \qquad \delta g_R^b = T_3^b \sin^2\theta_R^b, \\ &\delta g_R^B = T_3^b \cos^2\theta_R^b, \qquad \delta g_R^{bB} = \tfrac{1}{2}\sin\theta_R^b\cos\theta_R^b. \end{aligned} \tag{49}$$

In the doublet top partner model, only the right-handed standard model-like singlets $\mathcal{T}_1^R$, $\mathcal{B}_1^R$ have Yukawa type mixing with the new quarks, and therefore only the interactions in the right-handed sector are modified. Finally, the Higgs couplings are given by

$$\begin{aligned}\mathcal{L}_2^h = &- c_{tt}\frac{m_t}{v}\bar t_L t_R h - c_{TT}\frac{M_T}{v}\bar T_L T_R h - c_{tT}\frac{m_t}{v}\bar t_L T_R h \\ &- c_{Tt}\frac{M_T}{v}\bar T_L t_R h - c_{bb}\frac{m_b}{v}\bar b_L b_R h - c_{BB}\frac{M_B}{v}\bar B_L B_R h \\ &- c_{bB}\frac{m_b}{v}\bar b_L B_R h - c_{Bb}\frac{M_B}{v}\bar B_L b_R h + \text{H.c.},\end{aligned} \tag{50}$$

where

$$\begin{aligned} &c_{tt} = \cos^2\theta_R^t, \qquad c_{TT} = \sin^2\theta_R^t, \\ &c_{tT} = c_{Tt} = \sin\theta_R^t\cos\theta_R^t, \qquad c_{bb} = \cos^2\theta_R^b, \\ &c_{BB} = \sin^2\theta_R^b, \qquad c_{bB} = c_{Bb} = \sin\theta_R^b\cos\theta_R^b. \end{aligned} \tag{51}$$

The derivation of these couplings follows the lines of Eq. (25), just with

$$v H_{(2),ks}^t = M_{(1),ks}^t \delta_{s1}. \tag{52}$$

### B. Experimental limits on doublet fermion model

The decay $Z \to b\bar b$ puts a strong restriction on $\sin\theta_b^R$ since mixing in the right-handed $b$-quark sector contributes to $\delta g_R^b$ at tree level,

$$\delta g_R^b = -\tfrac{1}{2}(\sin\theta_R^b)^2. \tag{53}$$

From Eq. (10), the mixing angle in the right-handed $b$ sector is highly constrained,

$$|\sin\theta_R^b| < 0.115. \tag{54}$$

The contribution to $\delta g_L^b$ in the left-handed sector occurs at one-loop. Subtracting out the standard model contribution, in the limit $x, x' \gg 1$, the approximate result in the doublet fermion model is [34]

$$\begin{aligned}\delta g_L^b = &\frac{g^2}{64\pi^2}\{\sin^2(\theta_L^t - \theta_L^b) f_1(x,x') \\ &+ (\sin\theta_R^t)^2\cos^2(\theta_L^t - \theta_L^b) f_3(x,x')\},\end{aligned} \tag{55}$$

where $f_1(x,x')$ is defined in Eq. (35) and

$$f_3(x,x') = -x + \frac{3}{2}\left(1 + \frac{x}{x'}\right) + \left(\frac{x'+x}{2} - 3\right)\frac{x}{(x'-x)}\log\left(\frac{x'}{x}\right). \tag{56}$$

In Fig. 9, we scan over $\sin\theta_R^b$ and $\frac{\delta}{M_T}$ and use the relationships of Eq. (44) to find the remaining parameters. We use the exact one-loop result for $\delta g_b^L$ following Refs. [34,74], and determine the 95% confidence level upper bound on $\frac{\delta}{M_T}$. Because of the tree level mixing in the $b$ sector in this model, along with the relationships of Eq. (44), the heavy fermions are required to be approximately degenerate, as is clear from Fig. 9. This result is relatively insensitive to $M_T$.

Since $\sin\theta_R^b$ is constrained to be quite small, we will consider the oblique parameters in the limit $\theta_R^b = 0$. From Eq. (44), $\theta_R^b = 0$ implies $\theta_L^b = 0$ and the free parameters are $m_t, m_b$, $M_T$, and $M_B$. Our results will always be

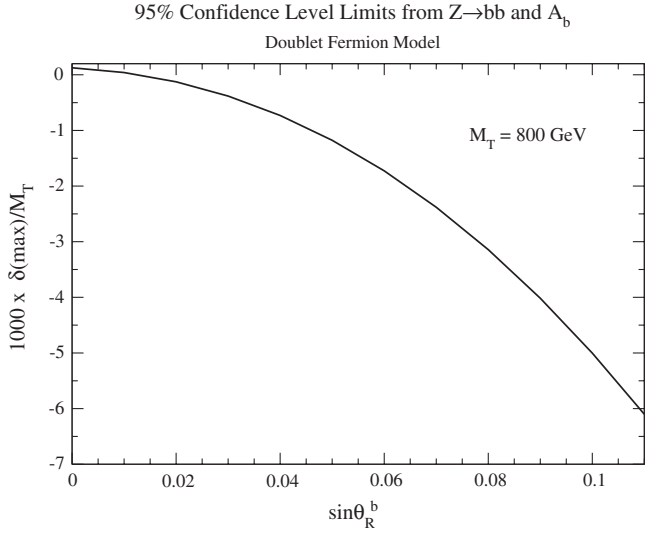


FIG. 9. Maximum value of $\frac{\delta}{M_T}$ allowed at the 95% confidence level from $R_b$ and $A_b$ as a function of $\sin\theta_R^b$ in the doublet fermion model.

expressed in terms of $\delta \equiv M_T - M_B$. In the $\theta_R^b = 0$, $m_b \to 0$ limit, the oblique parameters are well approximated by [69,76]

$$\Delta T_F(\text{approx}) = 4T_{\text{SM}}\frac{\delta}{M_T}\left[2\log(r) - 3 + \frac{5\log(r) - 3}{r}\right],$$
$$\Delta S_F(\text{approx}) = \frac{N_C}{9\pi}\frac{\delta}{M_T}\left[4\log(r) - 7 + \frac{4\log(r) + 7}{r}\right],$$
$$\Delta U_F(\text{approx}) = \frac{N_C}{9\pi}\frac{\delta}{M_T}\left[3 + \frac{6\log(r) - 17}{r}\right], \quad (57)$$

and

$$\delta g_b^L = \delta g_b^{L,\text{SM}}\frac{\delta}{M_T}\left[\log(r) - 4 + 3\frac{\log(r) - 2}{r}\right]. \quad (58)$$

It is apparent that decoupling of the effects of the new fermions occurs in the isospin conserving limit, $\frac{\delta}{M_T} \to 0$. Note also that $\delta g_b^L$ changes sign for $M_T \simeq 7m_t$. The oblique parameters are shown in Fig. 10 for $\delta = 1$ GeV. As in the singlet model, $\Delta T_F \gg \Delta S_F, \Delta U_F$.

The limits coming from the oblique parameters are found from a global fit to $S$, $T$, and $U$ as described in Sec. III B. For $\theta_R^b = 0$, the 95% upper limit on the mass splitting, $\delta$, is shown in Fig. 11 as a function of $M_T$. For $M_H = 125$ GeV and $M_T \sim 1$ TeV, the experimental constraints on the oblique parameters require $\delta \lesssim 8$ GeV. As shown in Fig. 11, it is possible to compensate for the negative contribution to $T$ from a heavier Higgs boson by a larger mass splitting $\delta$, which generates a positive contribution to $\Delta T_F$. However, the limits from $A_b$ and $R_b$ in this model are much more stringent than those coming from the oblique parameters.

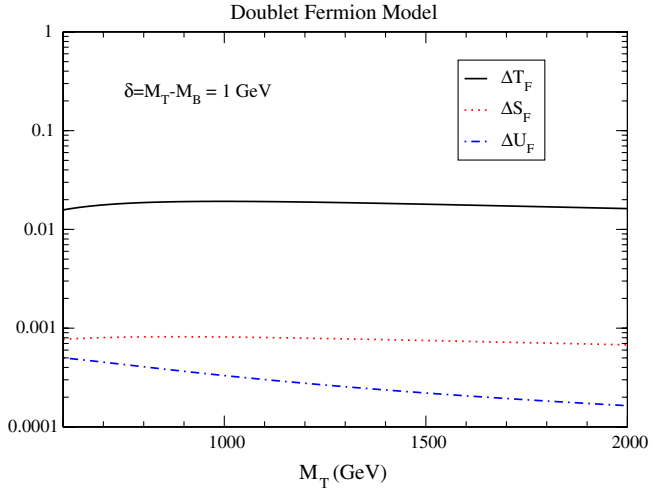


FIG. 10 (color online). Oblique parameters in the doublet fermion model in the limit $\theta_R^b = 0$ and $m_b \to 0$ as a function of $M_T$. We fix $\delta = M_T - M_B = 1$ GeV.

## VI. PHENOMENOLOGY

The new fermions affect the gluon fusion production rate, which at lowest order is given by [77–79]

$$\sigma(gg \to H) = \frac{\alpha_s^2}{1024\pi v^2}\,|\,\Sigma_q c_{qq} F_{1/2}(\tau_q)\,|^2\,\delta\left(1 - \frac{\hat{s}}{M_H^2}\right). \quad (59)$$

The sum is over $t$, $b$, $T$ in the singlet fermion model and over $t$, $b$, $T$, $B$ in the doublet model, the Yukawa couplings normalized to the standard model values $c_{qq}$ are given in Eqs. (23) and (51), and

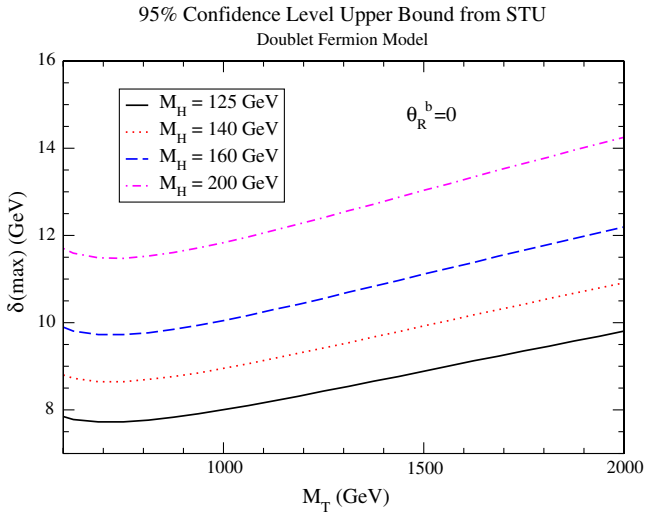


FIG. 11 (color online). Maximum mass splitting $\delta = M_T - M_B$ as a function of $M_T$ allowed at the 95% confidence level from the oblique parameters in the doublet fermion model for $\theta_R^b = 0$.

$$\tau_q = \frac{4M_q^2}{M_H^2}, \qquad F_{1/2} = -2\tau_q[1 + (1-\tau_q)f(\tau_q)],$$

$$f(\tau_q) = \begin{cases} \left[\sin^{-1}\left(\sqrt{\frac{1}{\tau_q}}\right)\right]^2, & \text{if } \tau_q \geq 1 \\ -\frac{1}{4}\left[\log\left(\frac{1+\sqrt{1-\tau_q}}{1-\sqrt{1-\tau_q}}\right) - i\pi\right]^2, & \text{if } \tau_q < 1. \end{cases} \quad (60)$$

We compute the gluon fusion production cross section through NNLO using the program IHIXS [8]. IHIXS allows the calculation of the cross section at NNLO for extensions of the standard model with an arbitrary number of heavy quarks having nonstandard Yukawa interactions [13], and puts the predictions on a firm theoretical basis. At NNLO, there are contributions that mix quark loops of different flavors (e.g. $t$ and $T$) and cannot be obtained by a simple rescaling of the lowest order cross section. We scan the parameter space allowed by the precision electroweak data as determined in the previous sections and discuss the maximum deviations from the standard model predictions.

### A. Top partner singlet model

The deviation from the standard model prediction of the NNLO Higgs production cross section as a function of the mixing angle in the top partner singlet model is shown in Fig. 12. The largest value of $\sin\theta_L$ allowed by the precision electroweak limits derived in Sec. IVA is also shown. As $\sin\theta_L$ increases, the mixing with the standard model-like top quark becomes significant, causing a suppression of the rate. This can be understood from the heavy mass limit ($m_t, M_T \gg \frac{M_H}{2}$) of the lowest order cross section, where the gluon fusion rate scales as

$$\frac{\sigma_{\text{Singlet}}}{\sigma_{\text{SM}}} \sim 1 - \frac{7}{60}\frac{M_H^2}{m_t^2}s_L^2\left(1 - \frac{m_t^2}{M_T^2}\right). \quad (61)$$

However, only the region to the left of the dot-dash line in Fig. 12 is allowed by the precision electroweak measurements, making the Higgs boson production rate in this model almost identical to the standard model rate. In contrast with composite [80] or little Higgs [59,81] models, which typically have a sizeable reduction of the Higgs production cross section relative to the standard model, in models with vector fermions the suppression is negligible because of the decoupling properties discussed in the previous sections. The uncertainty on the standard model cross section coming from scale, parton distribution function, and $\alpha_s$ uncertainties is roughly 15%–20% [7], so the extremely small deviation from the standard model prediction in the top partner singlet model is unobservable. The cross section for a heavier Higgs boson of mass $M_H = 300$ GeV is shown in Fig. 13. In this case, there is a region of mixing angles, $\sin\theta_L$, which is allowed by the precision electroweak measurements. Again, there is a slight, but unobservable, suppression of the NNLO rate relative to the standard model rate.

The loop-mediated Higgs decays to $\gamma\gamma$, $Z\gamma$, and $gg$ are also affected by the presence of top fermion partners. Figure 14 shows the deviation of the branching ratio to $\gamma\gamma$ from the standard model prediction. For small mixing, this deviation is always less than 1%.

### B. Top partner doublet model

The deviation from the standard model prediction for the NNLO gluon fusion cross section for Higgs production in

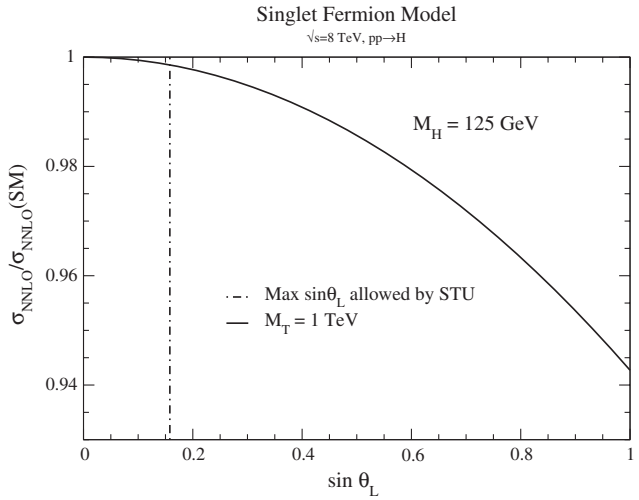


FIG. 12. The ratio of the NNLO Higgs cross section in the top partner singlet model normalized to the standard model prediction as a function of $\sin\theta_L$ for $M_H = 125$ GeV and $\sqrt{s} = 8$ TeV. The vertical line represents the maximum value of $\sin\theta_L$ allowed by electroweak precision measurements.

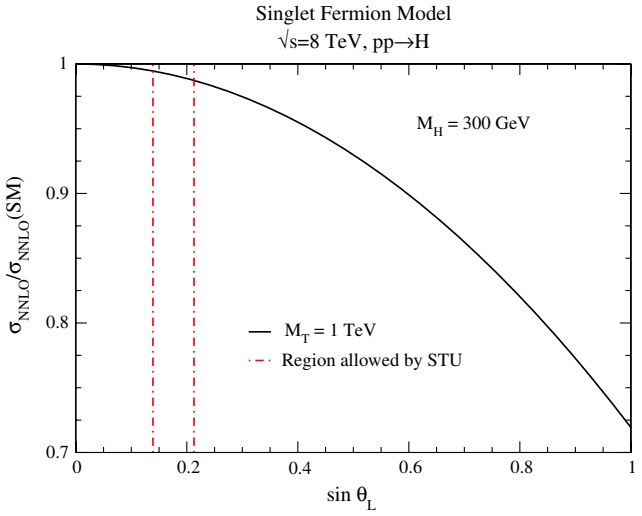


FIG. 13 (color online). The ratio of the NNLO Higgs cross section in the top partner singlet model normalized to the standard model prediction as a function of $\sin\theta_L$ for $M_H = 300$ GeV and $\sqrt{s} = 8$ TeV. The region between the vertical lines represents the region of $\sin\theta_L$ allowed by electroweak precision measurements.

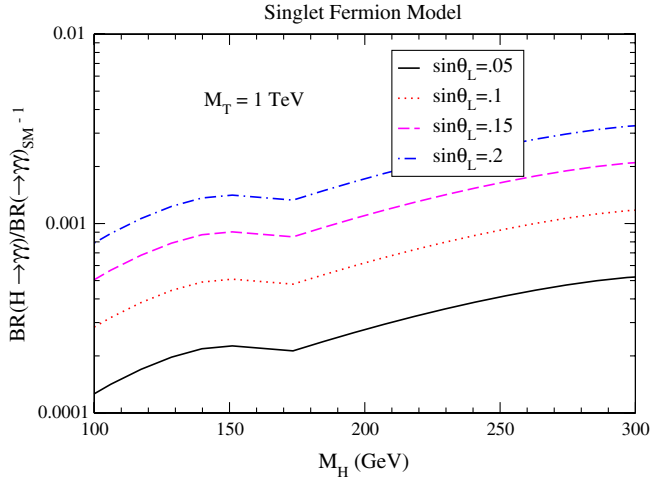


FIG. 14 (color online). Deviation of the $H \to \gamma\gamma$ branching ratio in the top partner singlet model from the standard model prediction.

the top partner doublet model (computed using IHIXS) is shown in Fig. 15. Also in this case the maximum difference from the standard model in the allowed regions of parameter space (Fig. 9) is always less than a few percent. This result can be understood by considering the heavy mass limit of the lowest order cross section for the gluon fusion production of the Higgs,

$$\frac{\sigma_{\text{Doublet}}}{\sigma_{\text{SM}}} \simeq (1+\sin^2\theta_R^b)\left[1+\sin^2\theta_R^b-\frac{7}{60}\frac{M_H^2}{m_t^2}\times\left(\frac{2r-1}{r}\sin^2\theta_R^b+\frac{2\delta}{M_T}-\frac{2\delta}{M_T}\frac{r+1}{r}\sin^2\theta_R^b\right)\right]. \tag{62}$$

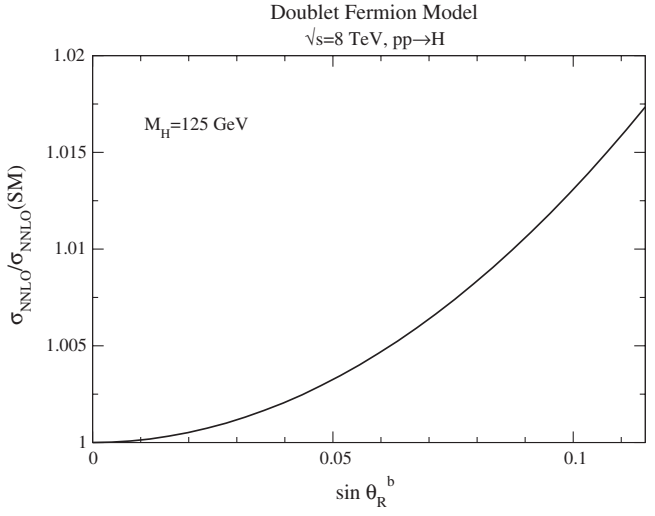


FIG. 15. The ratio of the NNLO Higgs cross section in the top partner doublet model normalized to the standard model prediction as a function of $\sin\theta_R^b$ for $M_H = 125$ GeV, $\sqrt{s} = 8$ TeV, and $M_T = M_B = 1$ TeV.

From the fits to $A_b$ and $R_b$, the maximum value of $\sin\theta_R^b$ is restricted to be 0.115, which implies

$$\frac{\sigma_{\text{Doublet}}}{\sigma_{\text{SM}}} \lesssim (1+\sin^2\theta_R^b)^2 \simeq 1.03. \tag{63}$$

Similarly, the deviations from the standard model in the Higgs decays to $\gamma\gamma$, $Z\gamma$, and $gg$ and in $H \to b\bar{b}$, which is affected at tree level, are not observable due to the small mixings and mass splitting allowed.

## VII. CONCLUSIONS

We have considered the effects on the gluon fusion Higgs boson production at NNLO from heavy vector quarks of charge $2/3$ and $-1/3$. Since the new quarks are vectorlike, their couplings to the Higgs boson are suppressed by mixing angles relative to the standard model Yukawa couplings. These mixing angles are restricted to be small by precision electroweak measurements. The most stringent bounds come from the oblique parameters for a vector singlet top partner, and from $A_b$ and $R_b$ for an extension of the standard model with an additional vector doublet. Because of the small mixing angles allowed, in these models the Higgs boson production rate as well as its decay branching ratios are essentially those of the standard model. The scenarios we have presented will be extremely difficult to disentangle from the standard model without the observation of direct production of the heavy fermions. Vector doublet fermions with a nonstandard hypercharge assignment are less restricted by precision electroweak measurements [36] and the mixing angles between the $t-b$ sector and the new fermion sector can be larger than in the cases we considered. However, even in this case, the low energy theorems for Higgs production require that the Higgs cross section approach the standard model result for large fermion masses.

If a Higgs boson is found at the LHC, attention will turn to understanding its properties. By performing global fits to the measured rates, information can be gleaned from the various cross section times branching ratio channels. For a light Higgs boson, it is likely that the dominant production channel will be gluon fusion, even in models with new physics. In this case, the rates are sensitive not only to a rescaling of the standard model couplings, but also to the effects of new particles that couple to the Higgs boson and contribute to the decay rates. Numerous preliminary attempts have been made to use current LHC data to discern differences from the standard model [81–90]. Our scenario with vector fermions demonstrates the difficulty of these indirect determinations of new physics—it is (un)fortunately not difficult to construct models that give Higgs signals indistinguishable from the standard model.

## ACKNOWLEDGMENTS

We would like to thank G. Panico for useful discussions. This work is supported by the United States Department of Energy under Grant No. DE-AC02-98CH10886.

## APPENDIX A: TWO-POINT FUNCTION FOR ARBITRARY FERMION COUPLING

The contributions to the gauge boson two-point functions from fermion loops parametrized by the interaction

$$\mathcal{L} = \bar{f}_1\left(C_{LX}^{f_1f_2}P_L + C_{RX}^{f_1f_2}P_R\right)\gamma_\mu f_2 V^\mu, \tag{A1}$$

for $V = W, Z, \gamma$ are [21,67]

$$\Pi_{XY} = -\frac{N_c}{16\pi^2}\left\{\frac{2}{3}\left(C_{LX}^{f_1f_2}C_{LY}^{f_1f_2} + C_{RX}^{f_1f_2}C_{RY}^{f_1f_2}\right)\left[m_1^2 + m_2^2 - \frac{p^2}{3} - (A_0(m_1) + A_0(m_2)) + \frac{m_1^2 - m_2^2}{2p^2}(A_0(m_1) - A_0(m_2))\right.\right.$$
$$\left.\left. + \frac{2p^4 - p^2(m_1^2 + m_2^2) - (m_1^2 - m_2^2)^2}{2p^2}B_0(m_1, m_2, p^2)\right] + 2m_1m_2\left(C_{LX}^{f_1f_2}C_{RY}^{f_1f_2} + C_{RX}^{f_1f_2}C_{LY}^{f_1f_2}\right)B_0(m_1, m_2, p^2)\right\} \tag{A2}$$

where

$$A_0(m) = \left(\frac{4\pi\mu^2}{m^2}\right)^\epsilon \Gamma(1+\epsilon)\left(\frac{1}{\epsilon} + 1\right)m^2, \qquad B_0(m_1, m_2, p^2) = \left(\frac{4\pi\mu^2}{m_2^2}\right)^\epsilon \Gamma(1+\epsilon)\left[\frac{1}{\epsilon} - f_1(m_1, m_2, p^2)\right], \tag{A3}$$

and

$$f_1(m_1, m_2, p^2) = \int_0^1 dx \log\left(x + \frac{m_1^2(1-x) - p^2x(1-x)}{m_2^2}\right). \tag{A4}$$

[1] A. B. Arbuzov, M. Awramik, M. Czakon, A. Freitas, M. W. Grunewald, K. Mönig, S. Riemann, and T. Riemann, Comput. Phys. Commun., **174**, 728 (2006).
[2] H. Flächer, M. Goebel, J. Haller, A. Hoecker, K. Mönig, and J. Stelzer (The Gfitter Group), Eur. Phys. J. C **60**, 543 (2009).
[3] S. Chatrchyan *et al.*, Phys. Lett. B **710**, 26 (2012).
[4] G. Aad *et al.*, Phys. Lett. B **710**, 49 (2012).
[5] Charalampos Anastasiou, Kirill Melnikov, and Frank Petriello, Phys. Rev. Lett. **93**, 262002 (2004).
[6] Robert V. Harlander and William B. Kilgore, Phys. Rev. Lett. **88**, 201801 (2002).
[7] LHC Higgs Cross Section Working Group, *Handbook of LHC Higgs Cross Sections: 1. Inclusive Observables*, edited by S. Dittmaier, C. Mariotti, G. Passarino, and R. Tanaka (CERN, Geneva, 2011).
[8] Charalampos Anastasiou, Stephan Buehler, Franz Herzog, and Achilleas Lazopoulos, J. High Energy Phys. 12 (2011) 058.
[9] Daniel de Florian and Massimiliano Grazzini, Phys. Lett. B **674**, 291 (2009).
[10] Charalampos Anastasiou, Radja Boughezal, and Frank Petriello, J. High Energy Phys. 04 (2009) 003.
[11] Charalampos Anastasiou, Radja Boughezal, and Elisabetta Furlan, J. High Energy Phys. 06 (2010) 101.
[12] Charalampos Anastasiou, Stephan Buehler, Elisabetta Furlan, Franz Herzog, and Achilleas Lazopoulos, Phys. Lett. B **702**, 224 (2011).
[13] Elisabetta Furlan, J. High Energy Phys. 10 (2011) 115.
[14] Graham D. Kribs, Tilman Plehn, Michael Spannowsky, and Timothy M. P. Tait, Phys. Rev. D **76**, 075016 (2007).
[15] Otto Eberhardt, Alexander Lenz, and Jurgen Rohrwild, Phys. Rev. D **82**, 095006 (2010).
[16] CMS Collaboration, combined results of searches for a Higgs boson in the context of the standard model and beyond-standard models.
[17] N. Arkani-Hamed, A. G. Cohen, E. Katz, and A. E. Nelson, J. High Energy Phys. 07 (2002) 034.
[18] Ian Low, Witold Skiba, and David Tucker-Smith, Phys. Rev. D **66**, 072001 (2002).
[19] Maxim Perelstein, Michael E. Peskin, and Aaron Pierce, Phys. Rev. D **69**, 075002 (2004).
[20] Spencer Chang and Jay G. Wacker, Phys. Rev. D **69**, 035002 (2004).
[21] Mu-Chun Chen and Sally Dawson, Phys. Rev. D **70**, 015003 (2004).
[22] Jay Hubisz, Patrick Meade, Andrew Noble, and Maxim Perelstein, J. High Energy Phys. 01 (2006) 135.
[23] Tao Han, Heather E. Logan, and Lian-Tao Wang, J. High Energy Phys. 01 (2006) 099.
[24] Christopher T. Hill, Phys. Lett. B **266**, 419 (1991).
[25] Christopher T. Hill and Elizabeth H. Simmons, Phys. Rep. **381**, 235 (2003).
[26] Bogdan A. Dobrescu and Christopher T. Hill, Phys. Rev. Lett. **81**, 2634 (1998).

[27] R. Sekhar Chivukula, Bogdan A. Dobrescu, Howard Georgi, and Christopher T. Hill, Phys. Rev. D **59**, 075003 (1999).

[28] Hong-Jian He, Timothy M. P. Tait, and C. P. Yuan, Phys. Rev. D **62**, 011702 (2000).

[29] Hidenori S. Fukano and Kimmo Tuominen, "A hybrid 4th generation: Technicolor with top-seesaw" (unpublished).

[30] Roberto Contino, Leandro Da Rold, and Alex Pomarol, Phys. Rev. D **75**, 055014 (2007).

[31] Marcela S. Carena, Eduardo Ponton, Jose Santiago, and Carlos E. M. Wagner, Nucl. Phys. **B759**, 202 (2006).

[32] Riccardo Barbieri, B. Bellazzini, Vyacheslav S. Rychkov, and Alvise Varagnolo, Phys. Rev. D **76**, 115008 (2007).

[33] Oleksii Matsedonskyi, Giuliano Panico, and Andrea Wulzer, "Light top partners for a light composite Higgs" (unpublished).

[34] P. Bamert, C. P. Burgess, James M. Cline, David London, and E. Nardi, Phys. Rev. D **54**, 4275 (1996).

[35] D. Comelli and Joao P. Silva, Phys. Rev. D **54**, 1176 (1996).

[36] Giacomo Cacciapaglia, Aldo Deandrea, Daisuke Harada, and Yasuhiro Okada, J. High Energy Phys. 11 (2010) 159.

[37] K. Nakamura *et al.* (Particle Data Group), J. Phys. G **37**, 075021 (2010).

[38] A. A. Akhundov, D. Yu. Bardin, and T. Riemann, Nucl. Phys. **B276**, 1 (1986).

[39] J. Bernabeu, A. Pich, and A. Santamaria, Phys. Lett. B **200**, 569 (1988).

[40] Wim Beenakker and Wolfgang Hollik, Z. Phys. C **40**, 141 (1988).

[41] C. P. Burgess, Stephen Godfrey, Heinz Konig, David London, and Ivan Maksymyk, Phys. Rev. D **49**, 6115 (1994).

[42] Howard E. Haber and Heather E. Logan, Phys. Rev. D **62**, 015011 (2000).

[43] ALEPH, DELPHI, L3, OPAL, SLD Collaboration, LEP Electroweak Working Group, SLD Electroweak Group, and Heavy Flavor Group Phys. Rep. **427**, 257 (2006); Reports No CERN-PH-EP/2005-041 and No. SLAC-R-774.

[44] Michael E. Peskin and Tatsu Takeuchi, Phys. Rev. D **46**, 381 (1992).

[45] Guido Altarelli and Riccardo Barbieri, Phys. Lett. B **253**, 161 (1991).

[46] Riccardo Barbieri, Alex Pomarol, Riccardo Rattazzi, and Alessandro Strumia, Nucl. Phys. **B703**, 127 (2004).

[47] M. Baak *et al.*, "Updated status of the global electroweak fit and constraints on new physics" (unpublished).

[48] W. Hollik, "Electroweak radiative corrections" (unpublished).

[49] Mu-Chun Chen, Sally Dawson, and C. B. Jackson, Phys. Rev. D **78**, 093001 (2008).

[50] Georges Aad *et al.*, "Search for pair production of a heavy quark decaying to a $W$ boson and a $b$ quark in the lepton + jets channel with the ATLAS detector" (unpublished).

[51] Georges Aad *et al.*, "Search for pair production of a new quark that decays to a $Z$ boson and a bottom quark with the ATLAS detector" (unpublished).

[52] Serguei Chatrchyan *et al.*, "Search for heavy, top-like quark pair production in the dilepton final state in $pp$ collisions at $\sqrt{(s)} = 7$ TeV" (unpublished).

[53] Serguei Chatrchyan *et al.*, "Search for heavy bottom-like quarks in 4.9 inverse femtobarns of $pp$ collisions at $\sqrt{(s)} = 7$ TeV" (unpublished).

[54] Serguei Chatrchyan *et al.* (CMS Collaboration), Phys. Rev. Lett. **107**, 271802 (2011).

[55] J. A. Aguilar-Saavedra, J. High Energy Phys. 11 (2009) 030.

[56] Christian J. Flacco, Daniel Whiteson, and Matthew Kelly, "Fourth generation quark mass limits in CKM-element space" (unpublished).

[57] Giacomo Cacciapaglia, Aldo Deandrea, Luca Panizzi, Naveen Gaur, Daisuke Harada, and Yasuhiro Okada, J. High Energy Phys. 03 (2012) 070.

[58] Keisuke Harigaya, Shigeki Matsumoto, Mihoko M. Nojiri, and Kohsaku Tobioka, "Search for the top partner at the LHC using multi-$b$-jet channels (unpublished).

[59] Joshua Berger, Jay Hubisz, and Maxim Perelstein, "A fermionic top partner: Naturalness and the LHC" (unpublished).

[60] J. A. Aguilar-Saavedra, Phys. Rev. D **67**, 035003 (2003).

[61] Monika Blanke, Andrzej J. Buras, Anton Poschenrieder, Cecilia Tarantino, Selma Uhlig, and Andreas Weiler, J. High Energy Phys. 12 (2006) 003.

[62] L. Lavoura and Joao P. Silva, Phys. Rev. D **47**, 1117 (1993).

[63] Marko B. Popovic and Elizabeth H. Simmons, Phys. Rev. D **62**, 035002 (2000).

[64] Tevatron Electroweak Working Group, Reports No. FERMILAB-TM-2427-E, No. TEVEWWG/top 2009/03, No. CDF Note 9717, and No. D0-NOTE-5899, 2009.

[65] Michael S. Chanowitz, M. A. Furman, and I. Hinchliffe, Nucl. Phys. **B153**, 402 (1979).

[66] S. Dawson and P. Jaiswal, Phys. Rev. D **82**, 073017 (2010).

[67] F. Jegerlehner, in *Testing the Standard Model*, edited by M. Cvetic and P. Langacker (World Scientific, Singapore, 1991), p. 476–590.

[68] G. Cynolter and E. Lendvai, Eur. Phys. J. C **58**, 463 (2008).

[69] Nobuhiro Maekawa, Phys. Rev. D **52**, 1684 (1995).

[70] Hong-Jian He, Christopher T. Hill, and Timothy M. P. Tait, Phys. Rev. D **65**, 055006 (2002).

[71] Csaba Csaki, D. Kribs, Patrick Meade, and John Terning, Phys. Rev. D **68**, 035009 (2003).

[72] Yang Bai, JiJi Fan, and JoAnne L. Hewett, "Hiding a heavy Higgs boson at the 7 TeV LHC" (unpublished).

[73] P. Bamert, "R($b$) and heavy quark mixing," (unpublished).

[74] Charalampos Anastasiou, Elisabetta Furlan, and Jose Santiago, Phys. Rev. D **79**, 075003 (2009).

[75] Marcela S. Carena, Eduardo Ponton, Jose Santiago, and C. E. M. Wagner, Phys. Rev. D **76**, 035006 (2007).

[76] L. Lavoura and Joao P. Silva, Phys. Rev. D **47**, 2046 (1993).

[77] Frank Wilczek, Phys. Rev. Lett. **39**, 1304 (1977).

[78] John R. Ellis, M. K. Gaillard, Dimitri V. Nanopoulos, and Christopher T. Sachrajda, Phys. Lett. **83B**, 339 (1979).

[79] H. M. Georgi, S. L. Glashow, M. E. Machacek, and Dimitri V. Nanopoulos, Phys. Rev. Lett. **40**, 692 (1978).

[80] Adam Falkowski, Phys. Rev. D **77**, 055018 (2008).

[81] Ian Low, Riccardo Rattazzi, and Alessandro Vichi, J. High Energy Phys. 04 (2010) 126.

[82] Bogdan A. Dobrescu, Graham D. Kribs, and Adam Martin, Phys. Rev. D **85**, 074031 (2012).
[83] Christoph Englert, Tilman Plehn, Michael Rauch, Dirk Zerwas, and Peter M. Zerwas, Phys. Lett. B **707**, 512 (2012).
[84] J. R. Espinosa, C. Grojean, and M. Muhlleitner, in Proceedings of Hadron Collider Physics Symposium 2011, Paris (unpublished).
[85] Dean Carmi, Adam Falkowski, Eric Kuflik, and Tomer Volansky, ''Interpreting LHC Higgs results from natural new physics perspective (unpublished).
[86] Aleksandr Azatov, Roberto Contino, and Jamison Galloway, J. High Energy Phys. 04 (2012) 127.
[87] J. R. Espinosa, Christophe Grojean, M. Muhlleitner, and Michael Trott, ''Fingerprinting Higgs suspects at the LHC'' (unpublished).
[88] Pier Paolo Giardino, Kristjan Kannike, Martti Raidal, and Alessandro Strumia, ''Reconstructing Higgs boson properties from the LHC and Tevatron data'' (unpublished).
[89] John Ellis and Tevong You, ''Global analysis of experimental constraints on a possible Higgs-like particle with mass 125 GeV'' (unpublished).
[90] Markus Klute, Remi Lafaye, Tilman Plehn, Michael Rauch, and Dirk Zerwas, ''Measuring Higgs couplings from LHC data'' (unpublished).